Atomic Force Microscope based Two-Dimensional Assembly of Micro/Nanoparticles

Afshin Tafazzoli[†] Chytra Pawashe[†] Metin Sitti[†*]

[†]Carnegie Mellon University
Mechanical Engineering Department
Pittsburgh, PA 15213, USA

[*]Carnegie Mellon University
Robotics Institute
Pittsburgh, PA 15213, USA

Abstract

This research aims at achieving two-dimensional micro/nanomanipulation and assembly of micro/nanoscale particles using Atomic Force Microscope (AFM). Unlike prior works, the presented manipulation models include friction models based on both the normal forces as well as the adhesion forces. Pull-off forces are modeled using the Johnson-Kendall-Roberts (JKR) contact mechanics model. This model is used to determine whether critical conditions for particle motion are achieved. Pushing manipulation experiments are performed on polystyrene microparticles. A top-view high resolution optical microscope, used for probe and particle position and motion detection, facilitated real-time visual feedback. A piezoelectric XYZ positioning stage with few nanometers precision enabled the two-dimensional precise assembly of the polystyrene microparticles. Using the real-time visual feedback, the behavior of particles manipulated by an AFM probe, is investigated. The results from the experiments matched those from the simulation, successfully verifying the developed models. The modeling, simulation and the experiments have enhanced the understanding of the interaction forces at the micro/nanoscale during micro/nanoassembly and particle manipulation.

1 Introduction

Recently, there has been great interest in exploring methods for assembly and manipulation at the micro/nanoscales to build miniaturized systems, devices, structures, and machines [1]-[3]. Controlled manipulation of micro/nanoparticles with atomic force microscope (AFM) probes has been investigated as a promising approach for micro/nano scale assembly [4]-[6]. The ability to precisely position micro/nano particles will enable the construction of novel micro/nanoscale electronic, optical, and quantum devices as well as novel materials, sensors, mechanisms, and machines. The range of applications of micro/nanoassembly in medicine, biology, chemistry, etc. is rapidly growing [7].

The AFM, though primarily used as an imaging tool with atomic resolution, is also evolving into a precision manipulation tool. Using AFM probe as a manipulation (pushing) tool enables precise particle positioning in a two-dimensional space for micro/nanoassembly [8]-[10]. Precise micro/nanoassembly is extremely important for electronic and optical device fabrication. Challenges due to the limitations in force and visual sensing capabilities can be overcome by advances in automatic manipulation and tele-manipulation [11], [12].

In this paper, a dynamic model of micro/nanoparticle behavior during manipulation has been developed. The model has enhanced the understanding of the manipulation and assembly procedure at the micro/nanoscale. The physics and governing equations in the macro-systems are different from the micro/nanosystems where adhesion forces and contact deformations are critical [13]-[15]. Micro/nanoadhesion forces are accounted in the model used to develop a real-time micro/nanomanipulation simulation. Its novelty is that the particle position can be traced at every instant. At the same time, all the particle motion dynamics and deformations are obtained from the numerical simulation accompanied by a real-time visual interface of the manipulated particle.

For micro/nanomanipulation and assembly purposes, the AFM tip makes contact with a micro/nanoparticle and moves the particle on the substrate (figure 1). After the non-contact mode scanning of the substrate and the targeted particles, the AFM tip approaches and makes contact with the target particle. The Contact angle φ is designed to be constant and greater than zero for pushing task. After the AFM tip comes into contact with the particle, the AFM probe starts to move with constant lateral velocity. The AFM deflections during pushing task can be sensed and recorded using a photodiode and optical methods. Lateral motion of the probe assists in increasing the AFM pushing force, F_T.

In this problem, both the substrate and the particle are stationary at the beginning. Then, the probe moves with a constat lateral velocity and pushing force reaches the critical force required to move the particle on the substrate. Therefore, the particle starts moving on the substrate and, based on the dynamic mode diagram of the particle [16], the suggested behavior follows. A microparticle is expected to roll on the substrate. The particle being pushed by the AFM probe moves with the same lateral velocity as the probe. This is used for high-precision positioning of micro/nanoparticles.

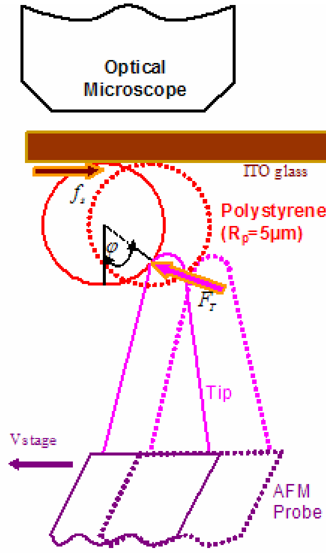

Figure 1: AFM tip moves polystyrene microparticle on the ITO glass substrate.

Micro/nanoobject manipulation/pushing using AFM is important for the following applications:

1. Micro/nanoassembly for electronic and optical device prototyping.
2. Micro/nanotribological characterization of materials by active pushing.
3. Real-time visualization during micro/nanomanipulation using graphical animation based on models and real-time force data.

2 Modeling

The AFM, which consists of a conical tip connected to a cantilever probe, is used as a manipulation tool for particle positioning. The AFM is modeled as a linear spring to account for normal deflection, and a torsional spring to record lateral twisting of the probe. Lateral deflection of the probe is not considered here as it is negligible. Spring coefficients of the springs in equation (1) are a function of the geometry and the mechanical properties. L, w, and t are the length, width, and thickness of the AFM probe, respectively. E and ν are the young's modulus and poison's ratio of the probe, respectively.

$$K_z = \frac{Ewt^3}{4L^3}$$
$$K_\theta = \frac{Ewt^3}{6L(1+\nu)} \tag{1}$$

Spring force and moment is a linear product of the spring constant and deflection. It is calculated in the "a-block" of the block diagram (figure 4). Spring force and moment (F_z, M_Θ), shear force (F_v), normal and lateral tip forces (F_Z, F_Y), and tip pushing force (F_T) are depicted during lateral movement of the particle in an AFM tip free-body diagram (figure 2). The unknown kinematics and dynamics are derived from the initial conditions and known inputs in the multi-dynamic positioning system. The positioning stage is moved with a constant lateral velocity, V_{stage}=constant. Assuming this velocity to be small, the quasi-static assumption can be considered to be valid ($d^2y_T/dt^2=0$). Thus the lateral position of the tip (y_T) and the torsional deflection of the probe (θ) can be defined as in (2).

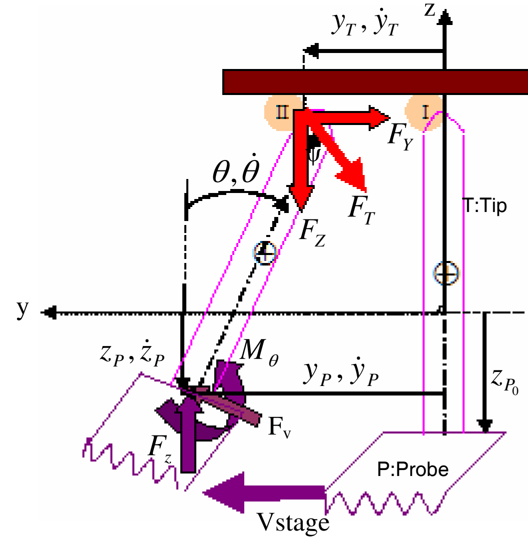

Figure 2: Free-body-diagram of the AFM tip and corresponding parameters.

$$\begin{aligned} y_T &= y_P - H\sin\theta \\ \dot{y}_T &= \dot{y}_P - H\dot{\theta}\cos\theta = Vstage - H\dot{\theta}\cos\theta \\ \ddot{y}_T &= -H\ddot{\theta}\cos\theta + H\dot{\theta}^2\sin\theta = 0 \Rightarrow \ddot{\theta} = \dot{\theta}^2\tan\theta \end{aligned} \tag{2}$$

where P corresponds to the probe and T to the tip. H is the tip height, and θ represents the angle of probe torsion. V_{stage} is the constant lateral velocity of the AFM probe stage.

The relation in equation (2) is used in the "a-block" of the block diagram to calculate torsional deflection of the probe at every instant. To determine the dynamics of the system, the normal deflection of the probe (Z_P) is critical and it is defined in (3).

$$\begin{aligned} z_P &= z_T - H\cos\theta \,;\; z_T = H + z_{P_0} = const. \\ \dot{z}_P &= H\dot{\theta}\sin\theta \\ \ddot{z}_P &= H\ddot{\theta}\sin\theta + H\dot{\theta}^2\cos\theta \end{aligned} \tag{3}$$

Therefore, forces on the AFM tip can be derived as in (4).

$$F_Z = \left(\frac{I_{(P)}\ddot{\theta} + M_\theta}{H}\right)\sin\theta + \left(F_z - \frac{m}{2}\ddot{z}_P\right)\cos^2\theta$$

$$F_v = \frac{1}{\sin\theta}(F_Z - F_z + \frac{m}{2}\ddot{z}_P) \quad (4)$$

$$F_Y = F_v \cos\theta$$

where $I_{(P)}$ is the moment of inertia of the AFM tip through its rigid contact with the probe, and m is the mass of the AFM tip. Above forces would determine the pushing force of the particle in (5).

$$F_T = \sqrt{F_Y^{\,2} + F_Z^{\,2}} \quad , \quad \psi = \tan^{-1}(F_Y / F_Z) \quad (5)$$

where ψ is the pushing force angle. From the pushing force magnitude (F_T) and the pushing force angle (ψ), the normal (F) and frictional forces (f) on the particle (figure 3) are derived in (6).

$$\begin{aligned} f_t &= F_T \cos\zeta \quad , \quad \zeta = \psi - \varphi - 90 \\ F_t &= -F_T \sin\zeta \\ f_s &= F_T \sin\psi \\ F_s &= F_T \cos\psi \end{aligned} \quad (6)$$

where t corresponds to the AFM tip and s to the substrate. φ is also the contact angle between the AFM tip and the particle.

Normal forces F_t and F_s would cause deformation on the tip-particle and the substrate-particle interfaces, respectively. Using the Johnson-Kendall-Roberts (JKR) model, the contact area (A) and the indentation depth (δ) on the substrate-particle interface are derived in (7).

$$A_s = \pi(a_s^{\,3})^{2/3} = \pi[\frac{R_{sp}}{K_{sp}}(F_s + 3\pi R_{sp}\omega_{sp} + \sqrt{6\pi R_{sp}\omega_{sp}F_s + (3\pi R_{sp}\omega_{sp})^2})]^{2/3}$$

$$\delta_s = \frac{a_s^{\,2}}{R_{sp}} - \frac{2}{3}\sqrt{3\pi\omega_{sp}a_s / K_{sp}} \quad (7)$$

In the above equations ω_{sp} is the interaction free energy, and K_{sp} is the equivalent modulus of elasticity of the substrate and the particle. Equivalent radius (R_{sp}) can be also derived as $R_{sp}=R_sR_p/(R_s+R_p)$ where R_s and R_p are the radii of the substrate and the particle. AFM tip is assumed to be spherical with the radius of R_t in contact with the spherical particle with the radius of R_p. In the "d-block" of the block diagram A, and δ are calculated both for the tip-particle and the substrate-particle interfaces.

According to the increase in the lateral pushing force and the contact deformation, frictional forces (f) in contact grow and reach their critical values (F^*). To determine these critical values, following tribological models are used for the sliding (8) and rolling (9) of the particle.

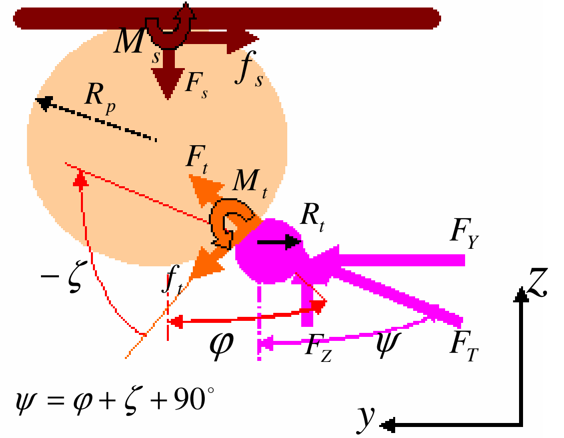

Figure 3: Forces during pushing a particle using AFM.

$$f_s > \mu F_s + \tau A_s \quad (8)$$

$$(f_s + f_t)R_p > M_s + M_t \;\; where \;\; M_s = \mu_r F_s + \tau_r A_s \quad (9)$$

where μ, μ_r are the friction coefficients, and τ, τ_r are the shear strengths of the surfaces in contact for sliding and rolling, respectively. Critical forces for sliding and rolling of the particle are derived in (10), (11).

$$F_s^{\,*} = \frac{\tau A_s}{\sin\psi - \mu\cos\psi} \quad (10)$$

$$F_r^{\,*} = \frac{\tau_r(A_s + A_t)}{R_p(\sin\psi + \cos\zeta) + \mu_r(\sin\zeta - \cos\psi)} \quad (11)$$

To avoid undesirable loss of contact due to the sliding on the tip or spinning of the particle, simulation parameters should be designed carefully. Comparing the pushing force with the critical forces, the behavior of the particle is determined. The "f-block" in the block diagram would account for these forces and specify the time when particle starts to move on the substrate.

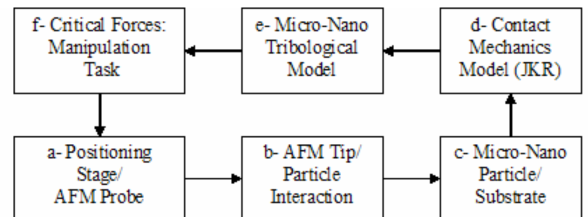

Figure 4: Block diagram for AFM based modeling of micro/nanoparticle manipulation (a-f blocks).

3 Simulations

5 µm radius polystyrene microsphere is pushed on the ITO glass substrate using AFM. Simulation parameters are as follows : $L=225\ \mu m$, $w=48\ \mu m$, $t=1\ \mu m$, $H=12\ \mu m$, $R_t=20\ nm$, $E=169\ GPa$, and $\upsilon=0.27$ as the AFM parameters, $\omega=0.1\ J/m^2$, and $K=5.48\ GPa$ as the contact mechanics (JKR) parameters, $\mu=0.8$, $\mu_r=80\ nm$, $\tau=28\ MPa$, and $\tau_r=28\ Pa.m$ as the tribological parameters, and $SimTime=30\ sec$, $V_{stage}=1\ \mu m/sec$, $R_p=5\ \mu m$, and $\varphi=45^\circ$ as the simulation parameters. Contact mechanics and tribological parameters can be obtained experimentally for different materials in contact.

The simulation is run for 30 seconds, and the nanopositioning stage is moved laterally with the constant velocity of 1 µm/sec. For alignment purposes, the AFM tip is brought into contact with the particle at the pre-defined contact angle ($\varphi=45^\circ$). After the simulation starts to run, the real-time visual interface helps us observe the manipulation procedure (figure 5). Especially in the nanoscale, where the microscope magnification is limited, this physical visual interface is of great importance.

From the following graphs obtained from the simulation, the applied pushing force, the time required for the particle to start moving on the substrate, and also the position of the particle at the end of simulation are derived (figures 6, 7).

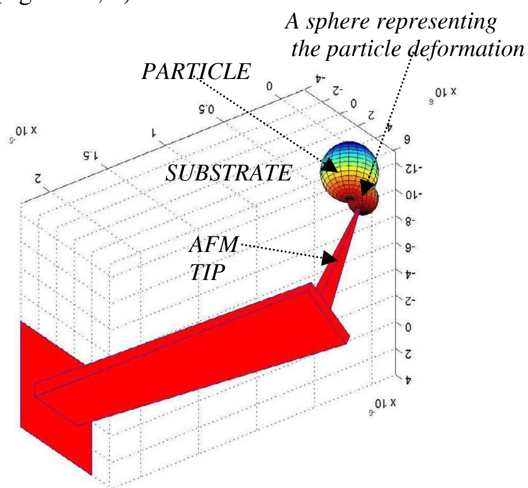

Figure 5: Real-time visual interface for pushing manipulation.

It is predicted that the pushing force increases to 3µN in 9 seconds, when it reaches the critical rolling force for the particle to start rolling on the surface. After 30 seconds, the particle was moved 21µm in the lateral direction.

4 Experiments

The micro/nanomanipulation system consists primarily of (figure 8): 1. A high powered light microscope with up to 1000x magnification (Nikon Eclipse L200), 2. a manual, coarse three-axis positioning stage, and 3. a three-axis nanopositioning stage.

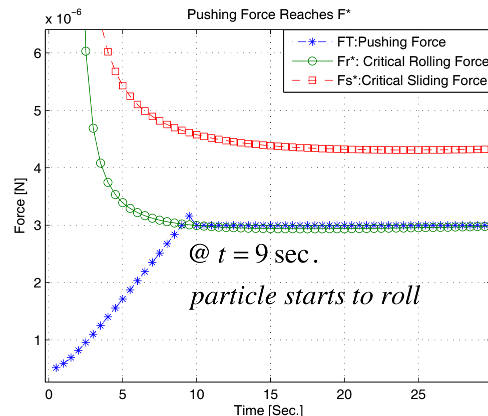

Figure 6: AFM pushing force meets particle critical rolling force and then stays constant.

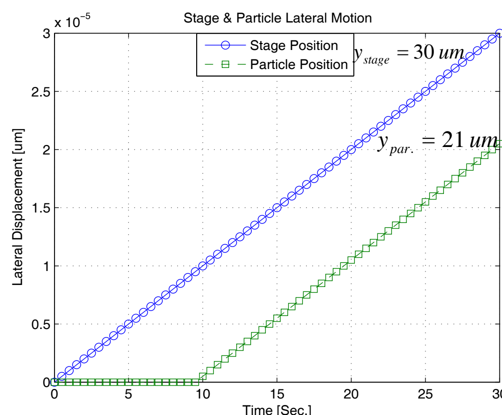

Figure 7: Stage and particle lateral position after 30 seconds ($V_{stage}=1\ \mu m/sec$).

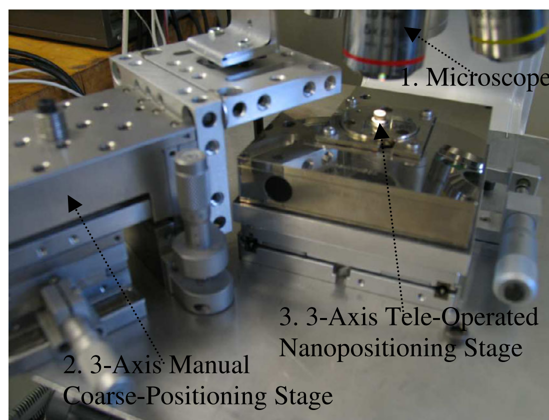

Figure 8: Micro/nanomanipulation system, 1. microscope 2. coarse-positioning 3. nanopositioning.

With the high-powered light microscope, particles in the upper nanoscale and microscale are visible. For manipulating particles with 500nm diameter, full visual feedback is feasible. To allow for the equipment to be placed under the microscope at high zoom levels, an inverted microscope setup was used. In this setup, a

transparent glass slide (ITO glass) is mounted on the coarse positioning stage. The samples are placed on the underside of the glass (since surface adhesion is much stronger at the micro and nano scale, the particles do not fall off). The manipulation AFM probe is mounted on the nanopositioning stage below the glass slide, pointing upwards (figure 10.a). Thus, in this setup, it is possible to visualize both of the micro and large nanoscale particles during manipulation as well as the tip-particle interaction. This is particularly advantageous when AFM probes are used. Since the tip is on the underside of an AFM probe, the tip-particle contact is usually hidden from view. With this inverted microscope setup, the tip-particle contact can be observed.

The nanopositioning stage has a range of 100 µm in the x and y axes, and a range of 15 µm in the z axis. With the system on an air isolation platform, the x and y axes have ±10 nm precision, and the z-axis has ±2 nm precision. With these precisions, this setup can support nanoscale manipulation. Control of the nanopositioning stage is achieved through a digital interface from PC using custom real-time scheduling software. The stage can be manipulated interactively, for example, by using a mouse or keyboard in real-time.

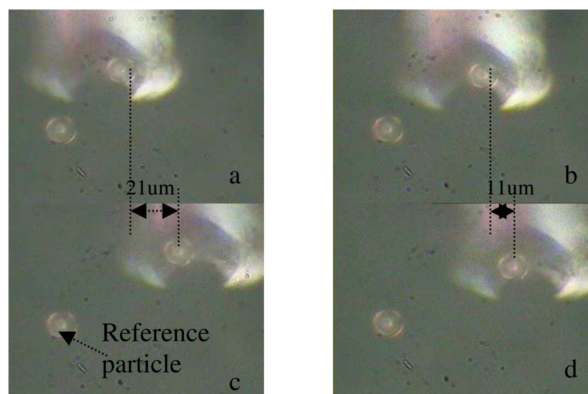

Figure 9: Position of the particle before and after being pushed by AFM tip. a, b. before c, d. after. a, c. $\varphi=45^\circ$ b, d. $\varphi=15^\circ$. $V_{stage}=1\ \mu m/sec$.

As shown in figure 9, the polystyrene particle is moved 21 µm in the lateral direction after 30 seconds (figure 9.c). The result from the experiment is in agreement with the simulation result, using the same parameters from simulation. The reference particle helped us measure the position of the moved particle before and after the pushing experiment. Reducing the contact angle from 45 to 15 degree, delayed the particle rolling time that caused particle to move from 21 to 11 µm after 30 seconds (figure 9.d). The demonstrated ability to precisely position one particle at a time, motivated the assembly of the 'CMU' arrangement.

To construct the 'CMU' arrangement with microparticles (figure 10), polystyrene microspheres with an average radius of 5 µm were deposited on an ITO glass slide from a water-based solution (the water evaporates afterwards). ITO glass was used as one of its sides is conductive, and thus it can be grounded. This removes any charge that is built up on the particles, making particle manipulation easier as electrostatic interactions are suppressed. The slide was placed in the micromanipulation system and a non-contact mode AFM tip was used as the particle manipulator. A non-contact mode tip offers higher rigidity over a contact mode tip. This is desired for particle manipulation, as the tip will deform less while manipulating particles.

Initially, the probe and particles are manually prepared and aligned using a coarse positioning stage. Once aligned, precise positioning is achieved through tele-operation from a PC. Due to the limited range of the nanopositioning stage, the coarse positioning stage is used to retrieve particles from outer areas into the working space.

During the first 30 minutes of manipulation, pushing particles is not particularly difficult. In constructing the letters 'CMU', the 'C' and 'M' were completed within 30 minutes. Typically, a particle is first collected and moved into the working space either by coarse or nano positioning. Then it is slowly pushed until it is positioned. During pushing, the AFM probe will lose contact with the particle many times, so it requires multiple pushes to position a particle. This occurs due to the following two reasons: 1. the AFM probe deflects and brushes over the particle, losing contact, and 2. the particle will rotate around the AFM probe, losing contact with the axis of translation.

However after approximately 30 minutes, the manipulation world changes dramatically. After this time, the probe and particles tend to adhere with each other much more significantly than during the first 30 minutes. Manipulating and positioning particles is more difficult, and constructing the 'U' in the 'CMU' took hours. It is likely that the electrostatic forces on the probe have built up (possibly from rubbing against the particles) and are significant enough so that the probe and particles (which lie on a grounded ITO glass surface) stick, as the probe and particles become oppositely charged.

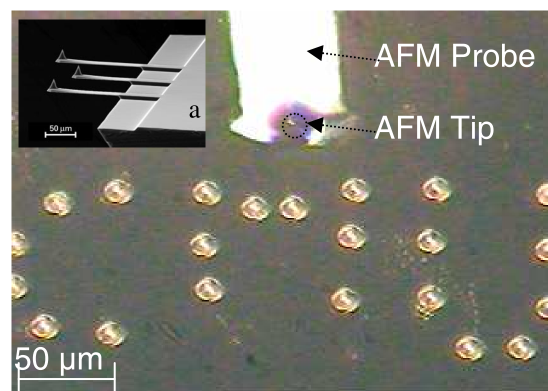

Figure 10: 'CMU' written with 10 µm polystyrene particles by AFM. a. SEM image of AFM.

5 Conclusions

In this paper, the complete model and simulation of micro/nanomanipulation has been devised based on preliminary modeling of the physics of small-scale particle motion dynamics. Particle positioning, using the AFM as a manipulator is modeled and dynamic behaviors of the particles are identified.

To obtain forces between the probe and particle, a real-time particle pushing simulation is developed. If the simulation continues to run for a known period of time, a new particle trace can be drawn which locates the new particle position. By controlling the stage velocity and mapping the location of particles at every instant, positioning of micro/nano particles can be achieved.

Designing simulation parameters not only achieves the desired dynamic performance to better understand real-time simulation, but they are also very effective tools for establishing valid experiments. Integrating the particle dynamics simulation with the experiment greatly benefits the furtherance of micro/nano assembly. Our simulation could be incorporated into manipulation tools to aid in precise kinematic and dynamic measurements. The results will be critical for the use of haptic interfaces for real-time manipulation of small-scale particles.

Acknowledgment

The authors wish to acknowledge the encouragement from all the NanoRobotics lab members at CMU and their invaluable feedback.

References

[1] M., Sitti, "Atomic Force Microscope Probe Based Controlled Pushing for NanoTribological Characterization," *IEEE/ASME Transaction on Mechatronics*, Vol. 9, No. 2, June 2004.

[2] G., Li, N., Xi, M., Yu, and W. K., Fung, "3-D Nanomanipulation Using Atomic Force Microscopy," *Proc. of ICRA'04*, Taipei, Taiwan, September 2003.

[3] M., Sitti, and H., Hashimoto, "Controlled Pushing of Nanoparticles: Modeling and Experiments," *IEEE/ASME Transactions on Mechatronics*, Vol. 5, No. 2, June 2000.

[4] T., Junno, K., Deppert, L., Montelius, and L., Samuelson, "Controlled Manipulation of Nanoparticles with an Atomic Force Microscope," *Appl. Physics Letters*, Vol. 66, pp. 3627-3629, June 1995.

[5] T. R., Ramachandran, C., Baur, A., Bugacov, and et al., "Direct and Controlled Manipulation of Nanometer-Sized Particles Using the Nan-Contact Atomic Force Microscope," *Nanotechnology*, Vol. 9, pp. 237-245, 1998.

[6] W., Zesch, and R. S., Fearing, "Alignment of Microparts Using Force Controlled Pushing," *SPIE Conf. on Microrobotics and Micromanipulation*, Boston, USA, November 1998.

[7] K., Laxminarayana, and N., Jalili, "A Review of Recent Developments in Atomic Force Microscopy Systems with Application to Manufacturing and Biological Processes", *Proc. of IMECE*, Washington, USA, November 2003.

[8] H., Miyazaki, and T., Sato, "Mechanical Assembly of Three-Dimensional Microstructures from Fine Particles," *Advanced Robotics*, Vol. 11, No. 2, pp. 169-185, 1997.

[9] D., Schafer, R., Reifenberger, A., Patil, and R., Andres, "Fabrication of Two-dimensional Arrays of Nanometer-Size Clusters with the Atomic Force Microscope," *Appl. Physics Letters*, Vol. 66, pp. 1012-1014, 1995.

[10] M., Sitti, and H., Hashimoto, "Two-Dimensional Fine Particle Positioning under Optical Microscope using a Piezoresistive Cantilever as a Manipulator," *Journal of Micromechatronics*, Vol. 1, No. 1, pp. 25-48, 2000.

[11] G., Li, N., Xi, M., Yu, and W. K., Fung, "Development of Augmented Reality System for AFM-Based Nanomanipulation," IEEE/ASME Transaction on Mechatronics, Vol. 9, No. 2, June 2004.

[12] M., Sitti, "Teleoperated and Automatic Manipulation Systems Using Atomic Force Microscope Probes," *Proc. of IMECE*, Washington, USA, November 2003.

[13] M. R., Falvo, R. M., Taylor, A., Helser, V., Chi, F. P., Brooks Jr, S., Washburn, and R., Superfine, "Nanometre-Scale Rolling and Sliding of Carbon Nanotubes", *Nature*, Vol. **397**, pp. 236-238, 1999.

[14] G., Dedkov, "Friction on the Nanoscale: New Physical Mechanism," *Meterials Letters*, Vol. 38, pp. 360-366, 1999.

[15] K. L., Johnson, "The Contribution of micro/nanotribology to the interpretation of dry friction," *Proc. of IMechE*, Vol. 214, Part C, 2000.

[16] A., Tafazzoli, and M., Sitti, "Dynamic Modes of NanoParticle Motion during Nanoprobe Based Manipulation", *Proc. of 4th IEEE Conf. in Nanotechnology*, Munich, Germany, August 2004.